

Corrosion Inhibition of Mild Steel by *Aloes* Extract in HCl Solution Medium

Hui Cang^{1,*}, Zhenghao Fei², Jinling Shao¹, Wenyang Shi¹, Qi Xu¹

¹ College of chemical engineering and biological, Yancheng institute of technology, Yancheng 224051, China

² Jiangsu Provincial Key Laboratory of Coastal Wetland Bioresources and Environmental Protection, Yancheng Teachers University, Yancheng 224002, China

*E-mail: Canghui_ycit@126.com; Canghui@ycit.edu.cn

Received: 27 October 2012 / Accepted: 22 November 2012 / Published: 1 January 2013

The corrosion inhibition of mild steel in 1.0 M HCl by the *Aloes* leaves extract has been studied using weight loss methods, potentiodynamic polarization and electrochemical impedance spectroscopy techniques. The results show that the inhibition efficiency increases with the increase of the extract concentration. The effect of temperature on the corrosion behavior of mild steel in 1M HCl with addition of the extract was also studied. The adsorption of the extract molecules on the steel surface obeys Langmuir adsorption isotherm and occurs spontaneously. The activation energy as well as other thermodynamic parameters for the inhibition process was calculated. These thermodynamic parameters show strong interaction between inhibitor and mild steel surface.

Keywords: Mild steel, Corrosion, Weight loss, Polarization, EIS

1. INTRODUCTION

Acid solutions are generally used for the removal of undesirable scale and rust in several industrial processes. Hydrochloric acid are widely used in the pickling processes of metals. Use of inhibitors is one of the most practical methods for protection against corrosion especially in acid solutions to prevent unexpected metal dissolution and acid consumption [1]. The use of organic compounds containing oxygen, sulphur and nitrogen to reduce corrosion attack on steel has been studied in the past decade [2-5]. The existing data show that most organic inhibitors get adsorbed on the metal surface by displacing water molecules and form a compact barrier film [6]. Availability of lone pairs and π electrons in inhibitor molecules facilitate electron transfer from the inhibitor to the

metal, forming a coordinate covalent bond [7]. The strength of the chemisorption bond depends on the electron density on the donor atom of the functional group and also the polarisability of the group.

Plant extracts are viewed as an incredibly rich source of naturally synthesized chemical compounds that can be extracted by simple procedures with low cost and are biodegradable in the environment. Entering into the 21st century, along with people's increasing awareness of protecting the environment, a large number of researches about plant leaves extracts as effective corrosion inhibitors of iron or steel in acidic media have been reported, such as *henna* [8], *Nypa fruticans* Wurmb [9], *Azadirachta indica* [10], *Acalypha indica* [11], *Zenthoxylum alatum* [12], *Damsissa* [13], *Phyllanthus amarus* [14], *Murraya koenigii* [15], *Justicia gendarussa* [16], *Oxandra asbeckii* [17], *Stevia rebaudiana* [18], *ginkgo* [19] and *Reed* [20] etc.. Through these studies, it is agreed that the inhibition performance of plant extract is normally ascribed to the presence in their composition of complex organic species such as tannins, alkaloids and nitrogen bases, carbohydrates, amino acids and proteins as well as hydrolysis products. These organic compounds contain polar functions with N, S, O atoms as well as conjugated double bonds or aromatic rings in their molecular structures, which are the major adsorption centers.

Aloes have abundant organic components in which N, S, O atoms are the main constituent atoms. These compounds involved, e.g. Aloemodin, Aloin-Barbaloin, Anthranol, Chrysophanol glucoside, Rutin etc.. However, it has never been studied in acid solutions for the purpose of the corrosion inhibition by *Aloes* extract. To explore this possibility, an attempt has been made to ascertain their corrosion inhibition properties. In present work inhibiting properties of the extract of *Aloes* in 1 M HCl were studied using weight loss method, and electrochemical methods.

2. EXPERIMENTAL

2.1 Preparation of plant extract

Dried *Aloes* (10g) plant leaves were soaked in deionized water (500ml) and refluxed for 5 h. The aqueous solution was filtered and concentrated to 100 ml. This concentrated solution was used to prepare solutions of different concentrations by dilution method. To obtain the mass of plant extract, it was dried at 100 °C under vacuum in the vaporizer. From the weight of the vacuum dried liquid, plant extract was found to contain 50 mg ml⁻¹ of plant compounds.

2.2 Weight loss method

Steel specimens of size 1 cm × 2.5 cm × 0.05 cm were used in weight loss experiments. Mild steel composed of (wt %) Fe 99.30%, C 0.076%, Si 0.026%, Mn 0.192%, P 0.012%, Cr 0.050% and Ni 0.050% were pre-treated prior to the experiment by grinding with emery paper (grade 600, 800, 1000 and 1200) then cleaned with double distilled water, degreased with acetone and dried. After weighting accurately using digital balance with sensitivity of ±0.01 mg, the specimens were immersed in 250 ml test solutions. All the aggressive acid solutions were open to air. The measurements were performed at

30 °C (except for temperature effect) for 6 h (except for immersion time effect) without and with various amounts of inhibitors or 4 h in the temperature range 50-70 °C. After the elapsed time, the specimen was taken out, washed, dried and weighted accurately. All the tests were conducted in aerated 1 M HCl. All the experiments were performed in triplicate and average values were recorded. The concentration of inhibitor for weight loss and electrochemical study were taken in mg L⁻¹. The inhibition efficiency η_w (%) and surface coverage θ was determined by using the following equation:

$$\theta = \frac{w_0 - w_i}{w_0}$$

$$\eta_w(\%) = \frac{w_0 - w_i}{w_0} \times 100$$

Where w_i and w_0 are the weight loss value in presence and absence of inhibitor, respectively.

The corrosion rate (C_R) of mild steel was calculated using the relation:

$$C_R = \frac{87.6w}{AtD}$$

Where w is the corrosion weight loss of mild steel (mg), A is the area of the coupon, t is the exposure time (h) and D is the density of mild steel (g ml⁻¹).

2.3 Electrochemical measurements

Electrochemical experiments were carried out in a conventional three-electrode cell with a platinum counter electrode (CE) and a saturated calomel electrode (SCE) coupled to a fine Luggin capillary as the reference electrode. To minimize the ohmic contribution, the tip of Luggin capillary was kept close to working electrode (WE). The WE was embedded in Teflon holder using epoxy resin with an exposed area of 0.785 cm². Before measurement the electrode was prepared as described above (Section 2.2), and then immersed in test solution at open circuit potential (OCP) for 1 h to be sufficient to attain the stable state. All electrochemical experiments were carried out using CHI660B electrochemical workstation. Each experiment was repeated at least three times to check the reproducibility and the good reproducible results were reported.

The potential of potentiodynamic polarization curves was started from cathodic potential of -250 mV to anodic potential of +250 mV vs. OCP at a sweep rate of 1 mV s⁻¹. Inhibition efficiency η_p (%) is defined as:

$$\eta_p(\%) = \frac{i_{corr}^0 - i_{corr}}{i_{corr}^0} \times 100$$

Where i_{corr}^0 and i_{corr} are the corrosion current density values without and with inhibitor, respectively.

Electrochemical impedance spectroscopy (EIS) measurements were carried out at open-circuit potential over a frequency range of 0.1 Hz - 100 kHz. The sinusoidal potential perturbation was 5 mV in amplitude. Electrochemical data were obtained after 1 h of immersion with the working electrode at the rest potential, and all tests have been performed in non-de-aerated solutions under unstirred conditions. Electrochemical data were analyzed by a Zsimpwin 3.30 Demo Version software. The values of η are calculated by the charge transfer resistance as follows:

$$\eta_E(\%) = \frac{R_{ct} - R_{ct}^0}{R_{ct}} \times 100$$

Where R_{ct} and R_{ct}^0 are the charge transfer resistance in presence and absence of inhibitor, respectively.

3. RESULTS AND DISCUSSION

3.1 Weight loss measurements

The corrosion inhibitor efficiency of the plant extract was determined in a test solution of 1 M HCl on mild steel surface at various temperatures. Fig. 1 shows the corrosion rate and inhibition efficiency of mild steel exposed to 1 M HCl at 30, 50 and 70 °C in the absence and presence of plant extract. The data results obtained from the weight loss measurements for the mild steel are listed in Table 1. It is evident from these results that inhibition efficiency of mild steel increase on addition of plant extract.

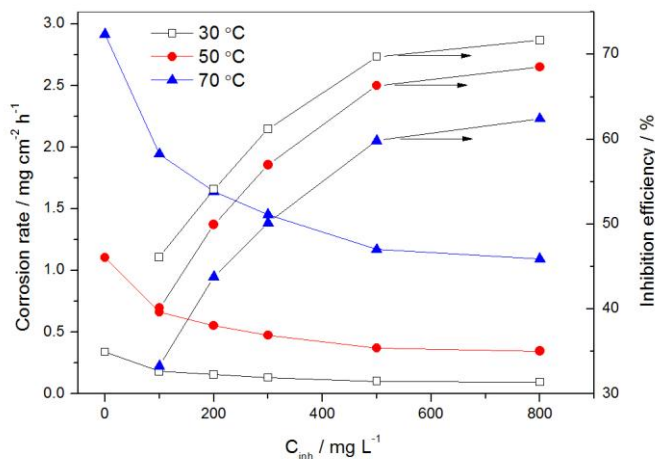


Figure 1. Corrosion rate and inhibition efficiency plots of mild steel immersed in 1 M HCl with and without the plant extract at 30, 50 and 70 °C.

Table 1. Weight loss data for mild steel in 1 M HCl without and with different concentrations of plant extract at various temperatures.

Concentration (mg L ⁻¹)	30°C			50°C			70°C		
	C_R (mg cm ⁻² h ⁻¹)	θ	η_w (%)	C_R (mg cm ⁻² h ⁻¹)	θ	η_w (%)	C_R (mg cm ⁻² h ⁻¹)	θ	η_w (%)
Blank	0.3406	-	-	1.1064	-	-	2.9192	-	-
100	0.1836	0.46	46.09	0.6625	0.4	40.12	1.9477	0.33	33.28
200	0.1563	0.54	54.10	0.5537	0.5	49.96	1.6409	0.44	43.79
300	0.1321	0.61	61.21	0.4761	0.57	56.97	1.4549	0.5	50.16
500	0.1031	0.70	69.72	0.3727	0.66	66.31	1.1721	0.6	59.85
800	0.0965	0.72	71.66	0.3481	0.69	68.54	1.0967	0.62	62.43

As the temperature increases, the corrosion rate increases and the inhibition efficiency decreases. The corrosion rate decreased and inhibition efficiency increased with increasing inhibitor concentration suggests that the inhibitor molecules act by adsorption on the metal surface. Consequently the increase of the inhibitor efficiency was ascribed to the increase in surface coverage. It is observed that corrosion inhibition efficiency decreased with temperature increasing and the best efficiency was obtained at 30°C as a result of a decrease in the adsorption of inhibitor molecules.

3.2 Potentiodynamic polarization

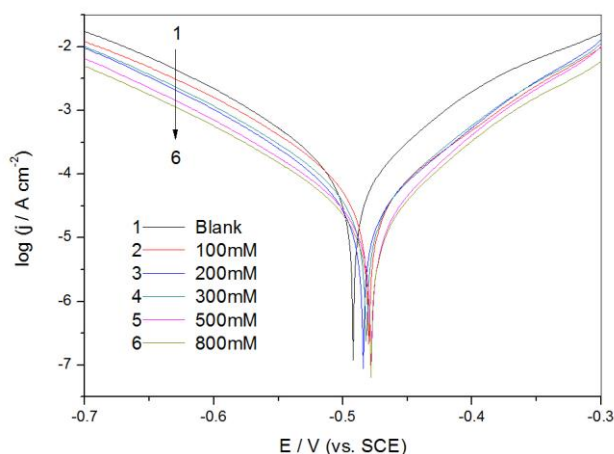


Figure 2. Potentiodynamic polarization curves for mild steel in 1 M HCl without and with different concentrations of the plant extract at 30°C.

Fig. 2 show potentiodynamic polarization curves for mild steel in 1 M HCl solutions without and with various concentrations of the plant extract. The electrochemical kinetic parameters, i.e.,

corrosion current densities (j_{corr}), corrosion potential (E_{corr}), cathodic Tafel slope (b_c) and anodic Tafel slope (b_a) are presented in Table 2. The inhibition efficiency (η_p) of the used extract in 1 M HCl is also given in Table 2.

E_{corr} values slightly shifted toward both positive and negative direction in the presence of different concentrations of the plant extract in 1 M HCl, indicating the inhibitor acted as a mixed type inhibitor [21]. However, it is clearly observed from Fig. 2 that the plant extract reduces the anodic and cathodic current densities, indicating the inhibition effects of the extract. In addition, from Table 2, the slope of the cathodic Tafel lines (b_c) and anodic Tafel lines (b_a) are observed to slightly change by the addition of the extract, which indicates the influence of the plant extract on the cathodic and anodic reactions, but the anodic curves are more affected. The data in Table 2 apparently showed that, the corrosion current densities decreased with increasing the inhibitor concentrations and the inhibition efficiencies increased.

Table 2. Potentiodynamic polarization parameters for the corrosion of mild steel in 1.0 M HCl solutions without and with various concentrations of plant extract at 30 °C.

Concentration (mg L ⁻¹)	E_{corr} (vs SCE/ V)	j_{corr} (mA cm ⁻²)	b_a (mV dec ⁻¹)	b_c (mV dec ⁻¹)	η_p (%)
Blank	-0.492	0.98	96.53	107.05	-
100	-0.480	0.538	88.05	106.25	45.05
200	-0.484	0.465	80.26	104.29	52.50
300	-0.482	0.397	85.49	106.11	59.45
500	-0.478	0.313	81.90	105.89	68.03
800	-0.478	0.286	84.95	108.31	70.79

3.3 Electrochemical impedance spectroscopy (EIS)

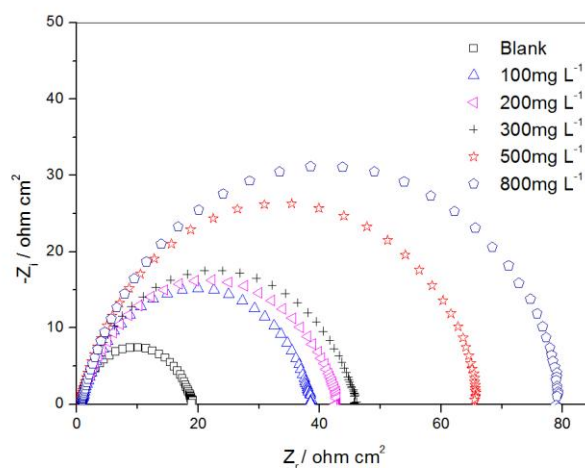


Figure 3. Nyquist plots for mild steel in 1 M HCl in the absence and presence of different concentrations of the plant extract.

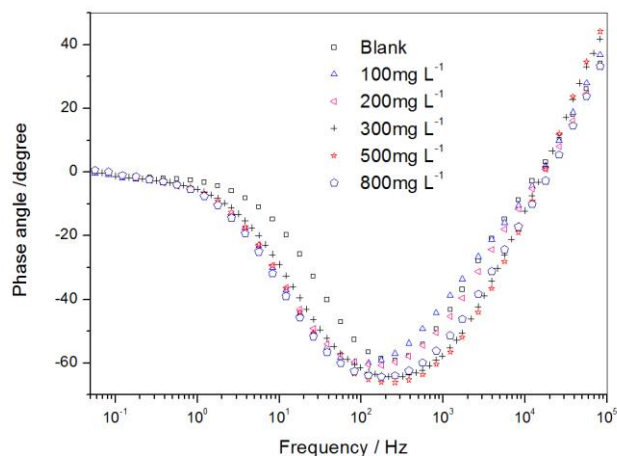


Figure 4. Bode plots of phase angle vs. frequency for mild steel in 1 M HCl in the absence and presence of different concentrations of the plant extract.

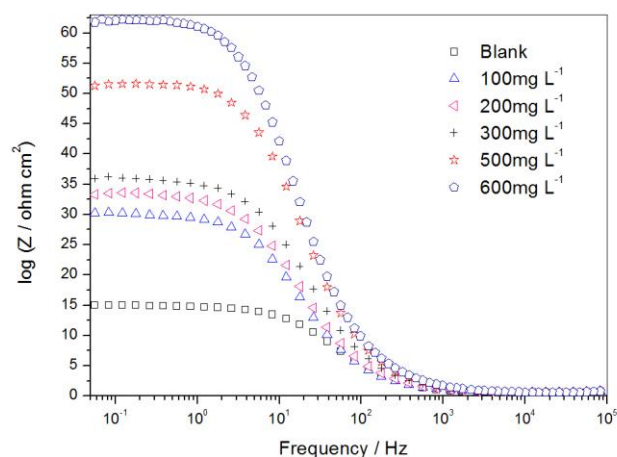


Figure 5. Bode plots of log Z vs. frequency for mild steel in 1 M HCl in the absence and presence of different concentrations of the plant extract.

The corrosion behavior of mild steel in 1 M HCl was also investigated by electrochemical impedance spectroscopy (EIS). Fig. 3 shows the Nyquist plots for mild steel in electrolyte solution in absence and presence of various concentrations of the plant extract at 30°C. Most of the impedance spectra obtained for the corrosion of mild steel in HCl solutions consists of either one depressed capacitive loop (one time-constant in Bode-phase representation) or two capacitive semicircles (two well-defined time-constants in Bode-phase format). The Bode plots of mild steel in 1 M HCl with and without the extract as shown in Fig. 4 and 5.

When the complex plane impedance (Nyquist plot) contains a “depressed” semicircle with the center under the real axis, such behavior characteristic for solid electrodes and often referred to as frequency dispersion, which have been attributed to roughness and inhomogeneity of the surface [22].

Two ways are used in the literature to describe the EIS spectra for the inhomogeneous films on the metal surface or rough and porous electrodes. One is the finite transmission line model [23] and the other is the filmed equivalent circuit model [24], which is usually proposed to study the degradation of coated metals [25]. It has been suggested that the EIS spectra for the metal covered by organic inhibitor films are very similar to the failed coating metals [26]. Therefore, in this work the filmed equivalent circuit model is used to describe the inhibitors-covered metal/solution interface. One time-constant in Bode-phase has been identified from Fig. 4 and 5, thus, the circuit model used for failed coating metal/solution interface is shown in Fig. 6.

When there is a non-ideal frequency response, it is common practice to employ distributed circuit elements in an equivalent circuit. The most widely used is the constant phase element (CPE), which has a non-integer power dependence on the frequency. Its impedance is described by the expression:

$$Z_{CPE} = Y^{-1}(i\omega)^{-n}$$

Where Y is a proportional factor; i is $\sqrt{-1}$; ω is $2\pi f$; and n is a phase shift.

Often a CPE is used in a model in place of a capacitor to compensate for non-homogeneity in the system. For $n=0$, Z_{CPE} represents a resistance with $R=Y^{-1}$, for $n=1$ a capacitance with $C=Y$, for $n=0.5$ a Warburg element and for $n=-1$ an inductance with $L=Y^{-1}$. Fig. 6 shows the electrical equivalent circuits employed to analyze the impedance plots. R_s is the electrolyte resistance ($\Omega \text{ cm}^2$), R_{ct} is the charge transfer resistance ($\Omega \text{ cm}^2$). Y ($\Omega^{-1} \text{ cm}^{-2} \text{ S}$) and n are parameters used in above-mentioned equation.

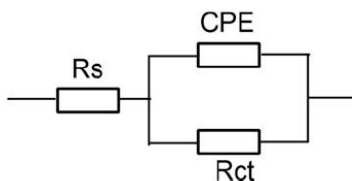


Figure 6. Equivalent circuit model used to fit the impedance spectra.

The impedance parameters derived from these plots are given in Table 3. The double layer capacitance (C_{dl}) and the frequency at which the imaginary component of the impedance is maximal (f_{max}) are found as represented in the following equation [27]:

$$C_{dl} = \frac{1}{2\pi f_{max} R_{ct}}$$

Where f_{max} is the frequency at which the maximum imaginary component of the impedance is obtained. Fig. 3-5 indicated that the corrosion process involved two step in any electrochemical process at the electrochemical interface, first, the oxidation of the metal (charge transfer process) and

second, the diffusion of the metallic ions from the metal surface to the solution (mass transport process). The plant extract gets adsorbed on the electrode surface and thereby produces a barrier for the metal to diffuse out to the bulk and this barrier increases with increasing the extract concentration.

Table 3. The impedance parameters obtained using equivalent circuit in Fig. 6 for mild steel in 1 M HCl solutions without and with various concentrations of the plant extract at 30°C.

Concentration (mg L ⁻¹)	R_s (Ω cm ²)	R_{ct} (Ω cm ²)	C_{dl} (μ F cm ⁻²)	η_E (%)
Blank	0.69	18.05	392	—
100	0.79	37.78	234	52.2
200	0.71	41.75	222	56.7
300	0.61	44.29	170	59.2
500	0.70	64.57	150	72.0
800	0.86	78.55	138	77.0

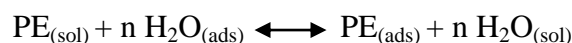
The data in Table 3 indicated that, as the extract concentration increased, the R_{ct} values increased but the C_{dl} values trend to decrease. The decrease in C_{dl} values generally related to the adsorption of organic molecules on the metal surface and then leads to a decrease in the local dielectric constant and/or an increase in the thickness of the electrical double layer [28].

$$\delta_{org} = \frac{\epsilon_0 \epsilon_r A}{C_{dl}}$$

Where δ_{org} is the thickness of the protective layer, ϵ_0 is the dielectric constant and ϵ_r is the relative dielectric constant. A low capacitance may result if water molecules at the electrode interface are largely replaced by the plant extract components through adsorption [29]. The results obtained from EIS are in good agreement with those obtained from potentiodynamic polarization methods.

3.4 Adsorption isotherm

The type of the adsorption isotherm can provide additional information about the properties of the tested compounds, and the adsorption depends on the compounds' chemical composition, the temperature and the electrochemical potential at the metal/solution interface. In fact, the water molecules could also adsorb on metal/solution interface. Thus, the so-called adsorption can be regarded as a quasi-substitution process between the plant extract in the aqueous phase [PE_(sol)] and water molecules at the electrode surface [H₂O_(ads)]:



Where $PE_{(sol)}$ and $PE_{(ads)}$ are the plant extract dissolved in the aqueous solution and adsorbed onto the metallic surface, respectively.

According to Langmuir adsorption isotherm, θ is related to equilibrium adsorption constant (K_{ads}) and C_{inh} by the equation:

$$\frac{C_{inh}}{\theta} = \frac{1}{K_{ads}} + C_{inh}$$

Fig. 7 shows the straight lines of C_{inh}/θ vs. C_{inh} at different temperatures. The parameters obtained from C_{inh}/θ vs. C_{inh} plots were listed in Table 4. These results show that all the linear correlation coefficients (R^2) are almost equal to 1 and the slopes are close to 1, which confirmed that the adsorption of the plant extract on mild steel surface good obeyed Langmuir adsorption isotherm. Table 4 revealed that K_{ads} decreased with increasing temperature, which indicated that the plant extract is easily and strongly adsorbed onto the mild steel surface at lower temperature, however, the adsorbed extract tended to desorb from mild steel surface at higher temperature.

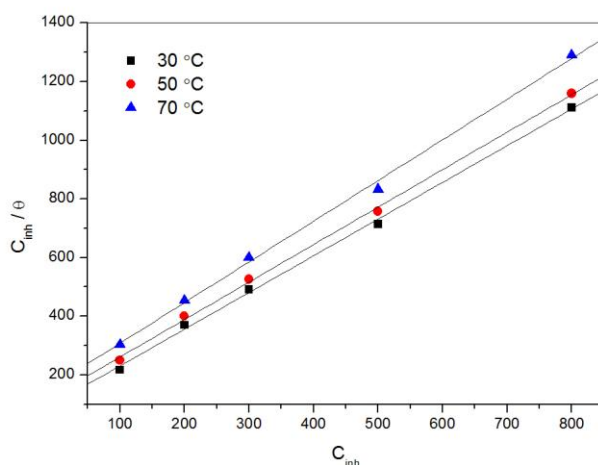


Figure 7. Langmuir’s adsorption plots for mild steel in 1 M HCl containing different concentrations of the plant extract at 30°C.

Table 4. The standard thermodynamic parameters of adsorption of the plant extract at different concentrations for mild steel in 1 M HCl solution.

Temp. (°C)	R^2	$10^3 K_{ads}$ (L mg ⁻¹)	ΔG°_{ads} (kJ mol ⁻¹)	ΔH°_{ads} (kJ mol ⁻¹)	ΔS°_{ads} (J mol ⁻¹ K ⁻¹)
30	0.997	9.489	-29.6	-10.20	64.03
50	0.998	7.527	-32.1		67.80
70	0.997	5.913	-34.4		70.55

3.5 Thermodynamic studies

Thermodynamic parameters play an important role in studying the inhibitive mechanism. The standard adsorption free energy (ΔG_{ads}°) was obtained according to [30]:

$$\Delta G_{ads}^{\circ} = -RT \ln(55.5K_{ads})$$

The thermodynamic parameters obtained are listed in Table 4. Generally, values of ΔG_{ads}° around -20 kJ mol^{-1} or lower are consistent with the electrostatic interaction between the charged molecules and the charged metal (physisorption); those around -40 kJ mol^{-1} or higher involve charge sharing or charge transfer from organic molecules to the metal surface to form a coordinate type of bond (chemisorption) [31]. The calculated ΔG_{ads}° value shows, therefore, that the adsorption mechanism of the extract on steel involves both two types of interaction. Indeed, due to the strong adsorption of water molecules on the surface of mild steel, one may assume that adsorption occurs first due to the physical force. The removal of water molecules from the surface is accompanied by chemical interaction between the metal surface and adsorbate, and that turns to chemisorptions [30]. In sum, the large negative values of ΔG_{ads}° reveal that the adsorption process takes place spontaneously and the adsorbed layer on the surface of mild steel is highly stable [32].

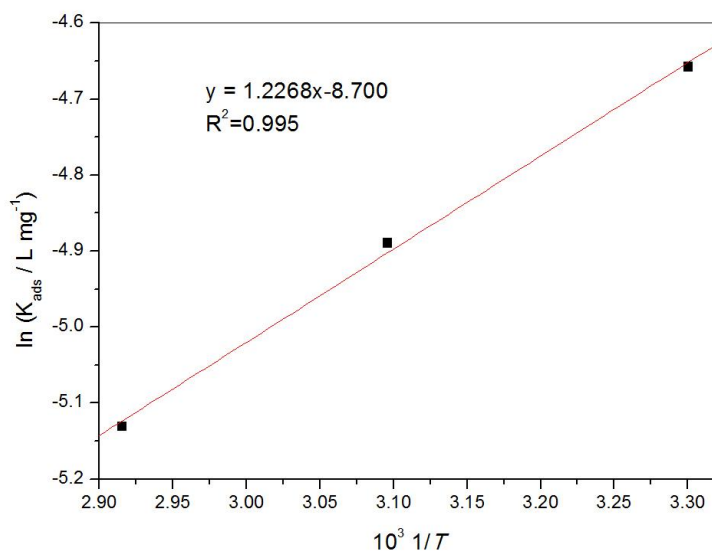


Figure 8. Langmuir's adsorption plots for mild steel in 1 M HCl containing different concentrations of the plant extract at 30°C.

It is worth noting that $-\Delta H_{ads}^{\circ}/R$ is the slope of the straight line $\ln K_{ads}$ vs. $1/T$ according to the Van't Hoff equation [33]:

$$\ln K_{ads} = -\left(\frac{\Delta H_{ads}^{\circ}}{RT}\right) + C$$

Where R is the gas constant ($R \approx 8.314 \text{ J K}^{-1} \text{ mol}^{-1}$), T is the absolute temperature, respectively. The straight line $\ln K_{ads}$ vs. $1/T$ is shown in Fig. 8. The adsorption heat ΔH_{ads} can be regarded as the standard adsorption heat ΔH_{ads}° because such experimental was carried out at the standard pressure and low solution concentration. The numerical value of ΔH_{ads}° was calculated in the Table 4. The negative sign of the standard adsorption heat indicated that the adsorption process of inhibitor is exothermic process, which illustrated that the corrosion inhibition efficiency decreased with the temperature increasing.

Thus, the standard adsorption entropy (ΔS_{ads}°) could be obtained by the following thermodynamic basic equation:

$$\Delta G_{ads}^{\circ} = \Delta H_{ads}^{\circ} - T\Delta S_{ads}^{\circ}$$

The positive values (in the Table 4) of ΔS_{ads}° suggested that the adsorption is coupled with an increase of the system disorder due to the adsorption of inhibitor on the steel surface. The temperature influences the rate of electrochemical progress as well as adsorption equilibration and kinetics. To evaluate the adsorption of the extract and activation parameters of the corrosion process of the mild steel in acidic media, temperature investigations allow the determination of activation energy, pre-exponential factor and other thermodynamic activation functions in absence and in presence of inhibitor. Arrhenius and the alternative formulation equations were used to elucidate the mechanism of corrosion inhibition [34,35]:

$$C_R = k \exp\left(-\frac{E_a}{RT}\right)$$

$$C_R = \frac{RT}{Nh} \exp\left(\frac{\Delta S}{R}\right) \exp\left(-\frac{\Delta H}{RT}\right)$$

Where E_a is the activation energy of the corrosion process, k is the pre-exponential factor, R the general gas constant, h is the plank's constant, N is Avogadro's number, ΔS is the apparent entropy of activation and ΔH is the apparent enthalpy of activation.

A plot of log of corrosion rate obtained by weight loss measurement vs. $1/T$ gave a straight line as shown in Fig. 9 with a slope of $-E_a/2.303R$. The values of activation energy are listed in Table 5. The higher values of E_a in presence of the plant extract than in its absence can be interpreted as an indication of adsorption effects. In presence of the inhibitor, the increased values of E_a , in general, reflected that the good ability to hinder the corrosion of mild steel in such conditions. In other words, the adsorption of the inhibitor on the electrode surface leads to the formation of a physical barrier that reduces the metal reactivity in the electrochemical reactions of the corrosion.

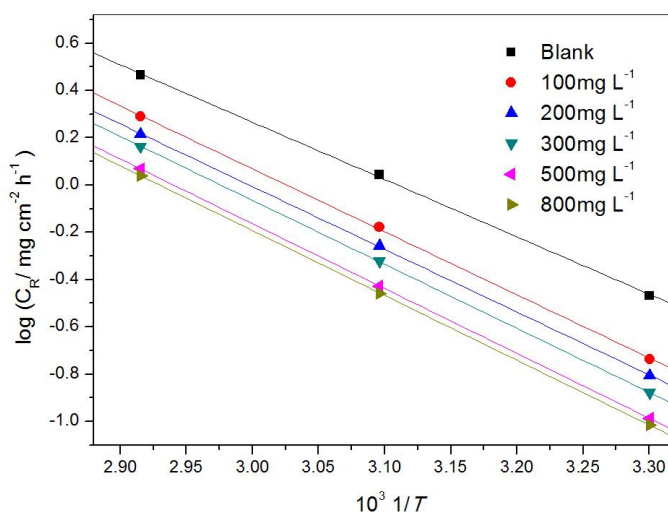


Figure 9. Arrhenius plots of $\log C_R$ vs. $1/T$ for mild steel in 1 M HCl containing different concentrations of the plant extract.

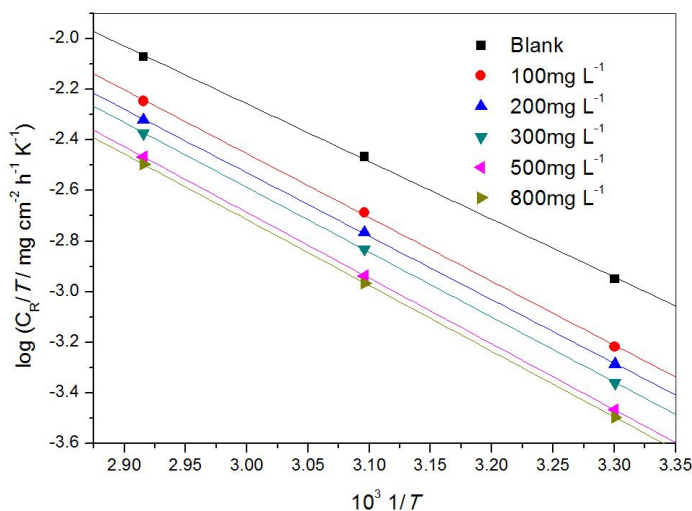


Figure 10. Arrhenius plots of $\log (C_R/T)$ vs. $1/T$ for mild steel in 1 M HCl without and with different concentrations of the plant.

A plot of $\log(C_R/T)$ vs. $1/T$ (Fig. 10) gave a straight line with the slope of $-\Delta H/2.303R$ and the intercept of $\log(R/Nh) + \Delta S/2.303R$, from which the values of ΔS and ΔH were calculated and given in Table 5. Inspection of these data reveals that the positive signs of enthalpy (ΔH) reflect the endothermic nature of dissolution process. The shift towards positive value of entropy (ΔS) imply that the activated complex in the rate determining step represents dissociation rather than association, meaning that disordering increases on going from reactants to the activated complex [36].

Table 5. Activation parameters for mild steel in 1 M HCl solution without and with different concentrations of the extract.

Concentration (mg L ⁻¹)	E_a (kJ mol ⁻¹)	$\Delta H_{\text{ads}}^{\circ}$ (kJ mol ⁻¹)	$\Delta S_{\text{ads}}^{\circ}$ (J mol ⁻¹ K ⁻¹)
Blank	46.45	43.77	-109.48
100	50.81	48.14	-99.45
200	51.05	48.37	-101.61
300	51.84	49.16	-99.63
500	52.50	49.82	-99.51
800	52.52	49.84	-100.09

4. CONCLUSIONS

The inhibition effect of the Aloes extract on mild steel in hydrochloric acid was examined by weight loss methods, potentiodynamic polarization and electrochemical impedance spectroscopy techniques. The results of inhibition efficiency determined by so-called measurements are in good agreement. Aloes extract acts as a good corrosion inhibitor in 1.0 M HCl solutions. Inhibition efficiency value increases with the increasing of the extract concentration, while the efficiency decreased with increasing the temperature. Polarization curves indicated that the extract acts as mixed type inhibitor in 1.0 M HCl solutions. EIS measurement results indicated that the resistance of the mild steel electrode increased greatly and its capacitance decreases by increasing the inhibitor concentration. The inhibition is accomplished by adsorption of the extract components on the iron surface, and the adsorption is spontaneous and obeys the Langmuir isotherm. The increase in E_a is proportional to the inhibitor concentration, indicating that the energy barrier for the corrosion interaction is also increased.

ACKNOWLEDGEMENT

This work was funded by the Applied Basic Research Project of Yancheng Institute of Technology (XKR2011005) and Jiangsu Beach Biological Resources and Environmental Protection of key Construction Laboratory Funding (JLCBE11002).

References

1. H. A. Sorkhabi, D. Seifzadeh and M. G. Hosseini, *Corros. Sci.*, 50 (2008) 3363.
2. L. M. Vracar and D. M. Drazic, *Corros. Sci.*, 44 (2002) 1669.
3. K. F. Khaled, *Appl. Surf. Sci.*, 230 (2004) 307.
4. M. Behpour, S. M. Ghoreishi, N. Soltani and M. Salavati-Niasari, *Corros. Sci.*, 51 (2009) 1073.
5. Y. M. Tang, X. Y. Yang, W. Z. Yang, R. Wan, Y. Z. Chen and X. S. Yin, *Corros. Sci.*, 52 (2010) 1801.
6. S. Muralidharan, K. L. N. Phani, S. Pitchumani, S. Ravichandran and S. V. K. Iyer, *J. Electrochem. Soc.*, 142 (1995) 1478.

7. N. Hackerman, R. M. Hard, Proc. Int. Congress of Metallic Corrosion, Butterworth, London (1962) 166.
8. A. Chetouani and B. Hammouti, *Bull. Electrochem.*, 19 (2001) 23.
9. K. O. Orubite and N.C. Oforika, *Mater. Lett.*, 58 (2004) 1768.
10. S. K. Sharma, A. Mudhoo, G. Tain and T. Sharma, *Green Chem. Lett. Rev.*, 3 (2010) 7.
11. M. Sivaraju and K. Kannan, *Inter. J. Chem. Tech. Res.*, 2 (2010) 1243.
12. L. R. Chuanhan and G. Gunasekaran, *Corros. Sci.*, 49 (2007) 1143.
13. A. M. Abdel-Gaber, B. A. Abd-El Nabey, I. M. Sidahmed, A. M. El-Zayady and M. Saadawy, *Corrosion*, 62 (2006) 293.
14. N. O. Eddy, *Electrochim. Acta*, 27 (2009) 579.
15. M. A. Quraishi, A. Singh, V. K. Singh, D. K. Yadav and A. S. Singh, *Mater. Chem. Phys.*, 122 (2010) 114.
16. A. K. Satapathy, G. Gunasekaran, S. C. Sahoo, K. Amit and R.V. Rodrigues, *Corros. Sci.*, 51 (2009) 2848.
17. M. Lebrini, F. Robert, A. Lecante and C. Roos, *Corros. Sci.*, 53 (2011) 687.
18. H. Cang, W. Y. Shi, J. L. Shao and Q. Xu, *Int. J. Electrochem. Sci.*, 7 (2012) 3726.
19. S. D. Deng, X. H. Li, *Corros. Sci.*, 55 (2012) 407.
20. H. Cang, Z. H. Fei, H. R. Xiao, J. L. Huang and Q. Xu, *Int. J. Electrochem. Sci.*, 7 (2012) 8869.
21. H. Cang, W. Y. Shi, Y. Lu, J. L. Shao and Q. Xu, *Asian J. Chem.*, 24 (2012) 3675
22. K. Juttner, *Electrochem. Acta*, 35 (1990) 1501.
23. J. R. Park and D. D. Macdonald, *Corros. Sci.*, 23 (1983) 295.
24. G. W. Walter, *Corros. Sci.* 30 (1990) 617.
25. G. W. Walter, *Corros. Sci.* 32 (1991) 1041.
26. F. Mansfeld, *Electrochem. Acta*, 35 (1990) 1533.
27. F. S. De Souza and A. Spinelli, *Corros. Sci.* 51 (2009) 642.
28. S. Martinez and M. Metikos-Hukovic, *J. Appl. Electrochem.*, 33 (2003) 1137.
29. M. Lebrini, M. Lagrenée, M. Traisnel and Gengembre L, *Appl. Surf. Sci.*, 253 (2007) 9267.
30. H. Cang, Z. H. Fei, W. Y. Shi and Q. Xu, *Int. J. Electrochem. Sci.*, 7 (2012) 10121.
31. K. F. Khaled and N. Hackerman, *Electrochim. Acta*, 49 (2004) 485.
32. M. Scendo and M. Hepel, *J. Electroanal. Chem.*, 613 (2008) 35.
33. T. P. Zhao, G. N. Mu, *Corros. Sci.* 41 (1999) 1937.
34. I. N. Putilova, S. A. Balezin and U. P. Baranik, *Metallic Corrosion Inhibitor*, Pergamon Press, New York, 1960, p. 31.
35. J. O'M. Bochriss and A. K. N. Reddy, *Modern Electrochemistry*, vol. 2, Plenum Press, New York, 1977, p. 1267.
36. K. R. Ansari, D. K. Yadav, E. E. Ebenso and M. A. Quraishi, *Int. J. Electrochem. Sci.*, 7 (2012) 4780.